MOLECULAR AND CELLULAR BIOLOGY, Sept. 1996, p. 5069–5080 Vol. 16, No. 9
0270-7306/96/$04.00+0


# The GTPase-Activating Protein *n*-Chimaerin Cooperates with Rac1 and Cdc42Hs To Induce the Formation of Lamellipodia and Filopodia

ROBERT KOZMA,[1,2] SOHAIL AHMED,[1,2] ANTHONY BEST,[1] AND LOUIS LIM[1,2]*

*Department of Neurochemistry, Institute of Neurology, London WC1N 1PJ, United Kingdom,[1] and Glaxo-IMCB Group, Institute of Molecular and Cell Biology, National University of Singapore, Singapore 0511[2]*

Received 12 February 1996/Returned for modification 26 March 1996/Accepted 22 May 1996

***n*-Chimaerin is a GTPase-activating protein (GAP) mainly for Rac1 and less so for Cdc42Hs in vitro. The GAP activity of *n*-chimaerin is regulated by phospholipids and phorbol esters. Microinjection of Rac1 and Cdc42Hs into mammalian cells induces formation of the actin-based structures lamellipodia and filopodia, respectively, with the former being prevented by coinjection of the chimaerin GAP domain. Strikingly, microinjection of the full-length *n*-chimaerin into fibroblasts and neuroblastoma cells induces the simultaneous formation of lamellipodia and filopodia. These structures undergo cycles of dissolution and formation, resembling natural morphological events occurring at the leading edge of fibroblasts and neuronal growth cones. The effects of *n*-chimaerin on formation of lamellipodia and filopodia were inhibited by dominant negative Rac1$^{T17N}$ and Cdc42Hs$^{T17N}$, respectively. *n*-Chimaerin's effects were also inhibited by coinjection with Rho GDP dissociation inhibitor or by treatment with phorbol ester. A mutant *n*-chimaerin with no GAP activity and impaired p21 binding was ineffective in inducing morphological changes, while a mutant lacking GAP activity alone was effective. Microinjected *n*-chimaerin colocalized in situ with F-actin. Taken together, these results suggest that *n*-chimaerin acts synergistically with Rac1 and Cdc42Hs to induce actin-based morphological changes and that this action involves Rac1 and Cdc42Hs binding but not GAP activity. Thus, GAPs may have morphological functions in addition to downregulation of GTPases.**

The Ras superfamily of GTPases plays an important role in regulating a variety of cellular processes (8, 18). These GTP-binding proteins have intrinsic GTPase and GDP/GTP exchange activities that can be regulated by associated proteins, such as GTPase-activating proteins (GAPs), GDP dissociation stimulators, and GDP dissociation inhibitors (GDIs). The activity of these proteins determines the cellular ratio of p21-GTP (on) to p21-GDP (off). In addition to regulating the p21-nucleotide state, these proteins may play other roles. For instance, Rho-GDI has been found in soluble complexes with RhoA, Rac1, and Cdc42Hs (28, 43) and has the ability to solubilize these proteins from membranes (24, 28), suggesting a role for it in recycling of Rho family proteins. Effector function has been proposed for the p120 Ras-GAP, as it is able to modulate muscarinic atrial potassium channel currents (34, 54). GAP domains are often found to be associated with other activities in complex proteins. Thus, there exist a novel myosin and a phospholipase C-activating protein, both of which contain Rho-GAP domains (23, 44); the Cdc42 and Rac1 GAP protein BCR also contains serine-threonine kinase activity (35), and the Cdc42 GAP protein RalBP1 also has binding activity to the p21 protein Ral (10).

Members of the Rho family include Cdc42, RhoA, and Rac1. Cdc42 was originally isolated as a yeast mutant defective in cell budding and polarity (1, 25). The human homolog, Cdc42Hs, complements the yeast Cdc42 mutant (38, 50). Similarly, yeast Rho proteins are thought to be required for cell polarity and budding maintenance (14). RhoA (37, 41, 45), Rac1 (46), and Cdc42Hs (27, 39) induce distinct changes in actin-based cell morphology when microinjected into mammalian cells. More specifically, RhoA induces focal adhesion assembly and stress fiber formation (41, 45), Rac1 induces lamellipodia and membrane ruffling and pinocytosis (46), and Cdc42Hs induces formation of filopodia (27, 39) and peripheral-actin microspikes (27). There is complexity in these signalling pathways as a consequence of cross-talk between Ras and the Rho family and between Rho family members. For example, Ras and Cdc42Hs induce membrane ruffling by activating the Rac1 pathway (27, 46) and Rac1 can induce stress fiber formation by activating the RhoA pathway (45).

*n*-Chimaerin (α1-chimaerin) is a 38-kDa GAP for Rac1 and Cdc42Hs whose activity in vitro is modulated by phorbol esters and phospholipids through its protein kinase C-like cysteine-rich domain (5). *n*-Chimaerin mRNA is expressed specifically in brain neurons and increases rapidly postnatally from birth to 20 days, a time of extensive cellular differentiation and synaptogenesis (19, 32). A related gene gives rise to β1-chimaerin, which has 77% protein sequence identity to *n*-chimaerin but is specifically expressed in the testes and localizes in germ cells during acrosomal assembly (30).

To determine its physiological function, we microinjected *n*-chimaerin or GAP domains into Swiss 3T3 fibroblast and N1E-115 neuroblastoma cells. We found that the GAP domain of *n*-chimaerin acts as a specific downregulator for the Rac1 pathway and works by stimulating its GTPase activity. However, microinjection of full-length *n*-chimaerin induced the formation of the actin-based structures lamellipodia and filopodia. Coinjection of *n*-chimaerin with dominant negative (T17N) mutant Rac1 or Cdc42Hs proteins, or with Rho-GDI, inhibited its function. Microinjected *n*-chimaerin colocalized with F-actin and caused a redistribution of the focal adhesion protein vinculin. *n*-Chimaerin will bind preferentially to GTPase-negative mutants of Rac1 and Cdc42Hs (6, 42). Together, these

* Corresponding author. Mailing address: Department of Neurochemistry, Institute of Neurology, 1 Wakefield St., London WC1N 1PJ, United Kingdom. Phone: 071-278-1552. Fax: 071-278-7045.

results suggest that *n*-chimaerin cooperates with Rac1 and Cdc42Hs in inducing changes in cytoskeletal morphology.

## MATERIALS AND METHODS

**cDNA subcloning into glutathione *S*-transferase and maltose-binding protein vectors, mutagenesis, and protein purification.** Rac1, Cdc42Hs, Rho-GDI, and GAP domain cDNAs subcloned into pGEX-2T as described previously (3, 6, 27) were used to express these proteins in *Escherichia coli*. In some cases cDNAs were subcloned into the derivative p265 or p265polyglycine to improve cleavage by thrombin. pGEX-2T derivatives p265 and p265polyglycine (17) have amino acid spacers between the thrombin cleavage site and the cDNA cloning site. *n*-Chimaerin full-length and N-terminal proteins were not expressed well in the glutathione *S*-transferase system, partitioning mainly into the insoluble fraction (3). However, when *n*-chimaerin cDNA was subcloned into p997, a maltose-binding protein fusion system, protein was completely soluble and expressed in high yield. For full-length *n*-chimaerin, the *Fok*I fragment (32) was purified and subcloned into the *Xmn*I site of p997. To obtain N-terminal protein, phorbol ester binding domain (amino acids 1 to 172), p997-*n*-chimaerin was cut with *Eco*RI and religated to remove the C-terminal domain. The full-length *n*-chimaerin mutants (Δ143–145 and Δ131–133) and C-terminal mutant (Δ1–105/Δ131–133) were generated and characterized as described elsewhere (6). For Rac1 and Cdc42Hs mutagenesis (G12V and T17N), a Clontech Transformer site-directed mutagenesis kit was used on cDNAs subcloned into pBluescript. After isolation, mutants were sequenced before being subcloned into p265 or p265polyglycine. For protein purification, *E. coli* cells carrying appropriate plasmids were grown to an optical density at 650 nm of 0.5 and 1 mM isopropyl-β-D-thiogalactopyranoside (IPTG) was added. Cells were harvested, resuspended in lysis buffer [10 mM sodium phosphate, 30 mM NaCl, 0.25% Tween, 10 mM β-mercaptoethanol, 2 mM EDTA, 2 mM ethylene glycol-bis(β-aminoethyl ether)-*N*,*N*,*N*′,*N*′-tetraacetic acid (EGTA)], and frozen at −20°C. When required, cells were thawed and sonicated (four times for 30 s each time, setting 4, MSE sonicator) and cell debris was removed by centrifugation at 14,000 × *g* for 10 to 20 min. Supernatants were then applied to glutathione-Sepharose or amylose columns and washed with 5 column volumes of the appropriate buffer (thrombin-containing buffer, or factor $X_a$-containing cleavage buffer, 1 mM phenylmethylsulfonyl fluoride, and a cocktail of protease inhibitors [2]).

Glutathione *S*-transferase fusion proteins were eluted with thrombin, and the thrombin was removed by using benzadiamine-Sepharose columns. For maltose-binding protein fusion proteins, elution was carried out with 10 mM maltose. Samples were then dialyzed, twice in 2 liters in factor $X_a$ buffer without maltose overnight to remove maltose, concentrated to approximately 2 mg/ml, and cleaved with factor $X_a$ buffer for 1 to 2 h at room temperature. Maltose-binding protein was removed by amylose chromatography. As *n*-chimaerin is a Zn metalloprotein, 50 μM zinc was added to the growth medium before induction with IPTG. Atomic-absorption analysis revealed that *n*-chimaerin and the phorbol ester binding domain were replete with zinc. All protein samples were more than 95% pure and frozen at −20°C in aliquots of 20 to 60 μl at 0.5 to 2.0 mg/ml.

**cDNA subcloning into the COS cell expression vector pMT2.** cDNAs coding for full-length rat and human *n*-chimaerin were subcloned into eukaryotic expression vector pMT2 (26) as follows. cDNAs encoding the rat C- and N-terminal portions of *n*-chimaerin (32) were ligated at the *Eco*RI sites, cut with *Hin*dIII, and cloned into Bluescript, generating RLAM 631. A *Pst*I fragment from RLAM 631, encoding full-length *n*-chimaerin, was ligated into the *Pst*I site of pMT2, generating pMT2-NC. A *Pst*I fragment encoding human *n*-chimaerin was subcloned from pBSCM1 (19) into the *Pst*I site of pMT2, generating pMT2-$NC^{\Delta 1-35}$. Finally, a deletion of the 0.6-kb *Eco*RI fragment from pMT2-NC yielded the construct pMT2-NTNC, which codes for the N-terminal amino acids 1 to 172 of *n*-chimaerin. Rat and human *n*-chimaerin are 97% identical at the amino acid level and indistinguishable in terms of biochemical activities. For all vectors used, cDNA constructs with opposite orientations were also prepared as controls. Standard DNA and cloning methods were employed as described by Sambrook et al. (48).

**Cell culture and transfection.** Swiss 3T3 and COS7 fibroblasts and N1E-115 neuroblastoma cells were cultured in Dulbecco's modified Eagle medium with 10% fetal calf serum (FCS) and antibiotic and antimycotic agents (Gibco) at 37°C with 5% $CO_2$. For transient transfection, COS7 cells were plated at $2 \times 10^5$ cells per 9-cm-diameter dish. The next day, medium was replaced, and 3 h later calcium phosphate-DNA precipitate was added. This DNA was prepared by adding 20 μg of plasmid DNA and 31 μl of 2 M $CaCl_2$ (made up to 250 μl) to 250 μl of 2× BES (2× BES is 50 mM BES [Calbiochem], 280 mM NaCl, and 1.5 mM $Na_2HPO_4$ [pH 6.95]). The precipitate was added to the cells for 16 h before a wash with normal medium. Cells were harvested 48 h after transfection.

**Cell fractionation and Western (immunoblot) analysis.** COS7 cell pellets were suspended in hypotonic buffer (20 mM Tris [pH 7.0], 10 mM KCl, 2 mM phenylmethylsulfonyl fluoride) on ice for 5 min and sonicated at high power three times for 5 s each time. Insoluble material was pelleted at 13,000 × *g* for 10 min, and the pellet was rewashed in hypotonic buffer. To investigate detergent solubility, cell pellets were resuspended in CSK buffer (140 mM NaCl, 10 mM Tris [pH 7.6], 2 mM phenylmethylsulfonyl fluoride, 1% Triton X-100). After incubation on ice for 5 min, the cytoskeleton was pelleted at 13,000 × *g* for 10 min and the pellet was rewashed. In all cases, soluble and insoluble fractions were finally resuspended in equivalent volumes of Laemmli buffer (29). Proteins were electrophoresed on 10% polyacrylamide–sodium dodecyl sulfate (SDS) gels and stained with Coomassie blue (0.1%) or electroblotted with a Sartoblot 11-S (Sartorius) onto nitrocellulose by using 25 mM Tris (pH 8.3)–192 mM glycine–20% methanol as transfer buffer. Prestained molecular weight markers were used (Sigma). Polyclonal rabbit antibodies to *n*-chimaerin were prepared as previously described (4). Western analysis was performed as follows. Nitrocellulose filters were blocked overnight at 4°C in 5% milk powder (Marvel), washed in phosphate-buffered saline plus 0.1% Tween (PBST), and incubated with anti-*n*-chimaerin polyclonal antibodies (diluted 200-fold in PBS). After a 1.5-h incubation at room temperature, five washes with PBST, incubation with peroxidase-conjugated anti-rabbit immunoglobulin G (Dako; diluted 1,000-fold in PBS), and five further washes in PBST, the filters were incubated with luminol enhanced chemiluminescence reagent (Amersham) and then exposed to Amersham Hyperfilm.

**Microinjection, in situ immunostaining, and lucifer yellow uptake.** Swiss 3T3 cells were grown on gridded glass slides. Subconfluent cells were starved in Dulbecco's modified Eagle medium plus 0.2% $NaHCO_3$ for 24 to 48 h before injection. Proteins were normally injected in 50 mM Tris-HCl (pH 7.5)–50 mM NaCl–5 mM $MgCl_2$–0.1 mM dithiothreitol by an Eppendorf microinjector and a Zeiss Axiovert microscope. Successful injection was determined visually at the time of injection and also by coinjection of the marker protein mouse immunoglobulin or *n*-chimaerin. Cell viability was estimated to be greater than 90%. For time-lapse studies, the cells were maintained on a heated platform (37°C) in a 10% $CO_2$ environment and viewed under phase contrast as described previously (28). For immunofluorescence staining, the cells were washed with PBS, fixed in 3% paraformaldehyde in PBS for 20 min, and washed in 0.2% Triton X-100 in PBS for 5 min. Fixed cells were incubated with 1:20-diluted antichimaerin ($4Ac^2$), antivinculin (Sigma), or anti-mouse immunoglobulin G (Dako) antibodies in PBS plus 3% bovine serum albumin (BSA) for 1.5 h at room temperature and then washed three times for 5 min each time in PBS. Then they were incubated with 1:100-diluted fluorescein isothiocyanate-conjugated anti-rabbit and anti-mouse antibodies (Dako) together with rhodamine-conjugated phalloidin (to stain filamentous actin; 0.2 mg/ml; Sigma) in PBS plus 3% BSA for 1 h, washed in PBS three times for 5 min each time, and mounted in Mowiol–1,4-diazabicyclo[2.2.2]octane (Aldrich). For determination of pinocytotic activity, microinjected log-phase Swiss 3T3 cells were incubated with 1 mg of lucifer yellow (Sigma) per ml for 1.5 h at 37°C before being washed in PBS and fixed with 3% paraformaldehyde. Cells were photographed under fluorescence with Ektachrome 400 film (Kodak).

## RESULTS

**The GAP domain of *n*-chimaerin inhibits the Rac1 signalling pathway.** The C-terminal GAP domain of *n*-chimaerin (amino acids 106 to 299) stimulates in vitro the GTPase activity of Rac1 (13) and with reduced potency that of Cdc42Hs but not that of RhoA (6, 33). Injection of this domain into fibroblasts resulted in the inhibition of both Rac1-induced membrane ruffling, identified after staining for filamentous actin with phalloidin (Fig. 1a and b), and pinocytosis as determined by lucifer yellow uptake (data not shown). In contrast, the N-terminal phorbol ester binding domain of *n*-chimaerin did not inhibit ruffling or pinocytosis (data not shown). Thus, the GAP domain acted as a cellular downregulator of the Rac1 pathway.

Coinjection experiments were carried out to establish how the GAP domain acted as a downregulator. The findings (data not shown) were as follows. Firstly, the GAP domain did not significantly reduce membrane ruffling induced by Rac1 complexed to GTP-γ-S (a nonhydrolyzable GTP analog). Secondly, a mutant GAP domain (Δ1–105/Δ131–133), which does not possess Rac1-GAP activity but does bind Rac1 (6), also did not reduce Rac1-mediated membrane ruffling. Thirdly, membrane ruffling induced by the GTPase-negative mutant $Rac1^{G12V}$ was not downregulated by the GAP domain. These results suggest that the GAP domain downregulates the Rac1 pathway by stimulating the Rac1 intrinsic GTPase activity.

The GAP domain acted specifically on the Rac1 pathway, as it did not affect the formation of structures induced by the RhoA or Cdc42Hs pathway, namely, stress fibers induced by 0.5% FCS or by lysophosphatidic acid (LPA) (Fig. 1c and d) and filopodia induced by bradykinin (27). These results show that the GAP domain of *n*-chimaerin is a useful reagent as a

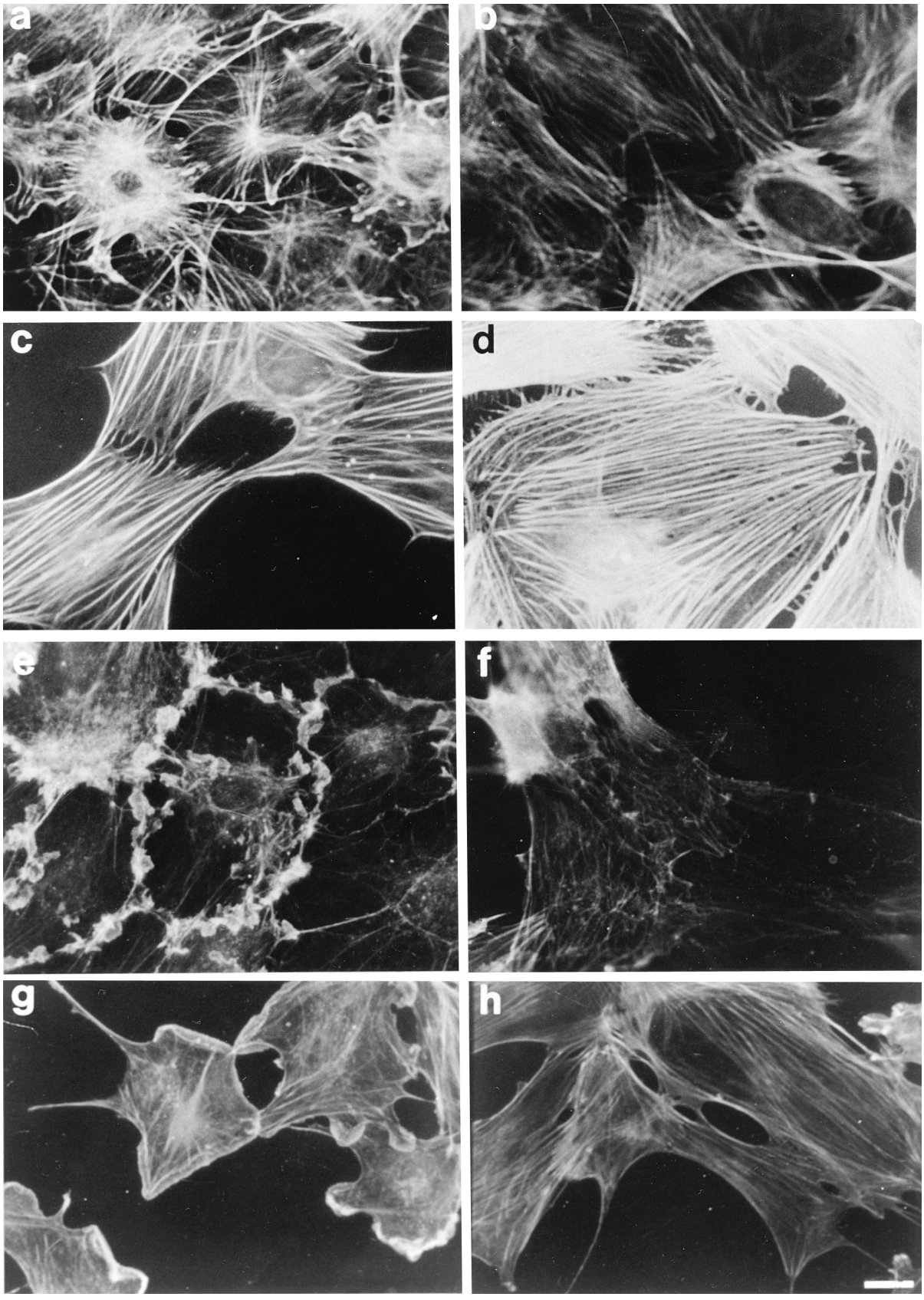


FIG. 1. The *n*-chimaerin GAP domain specifically downregulates the Rac1 pathway. (a and b) Serum-starved Swiss 3T3 cells microinjected with Rac1 protein (a) or Rac1 and GAP domain (Δ1–105) proteins (b); (c and d) cells treated with 20 ng of LPA per ml (c) and injected with GAP domain and then treated with LPA (d); (e and f) cells treated with 100 nM PMA (e) and injected with GAP domain and then treated with PMA (f); (g and h) cells treated with 1 μg of 1-oleyl-2-acetyl-rac-glycerol per ml (g) and injected with the GAP domain and then treated with 1-oleyl-2-acetyl-rac-glycerol (h). Cells were incubated for 10 min at 37°C after injections and/or treatments before fixation and staining with rhodamine-conjugated phalloidin. Proteins were each injected at 0.5 mg/ml. All cells in panels b, d, f, and h were microinjected with GAP domain protein. Bar, 10 μm.

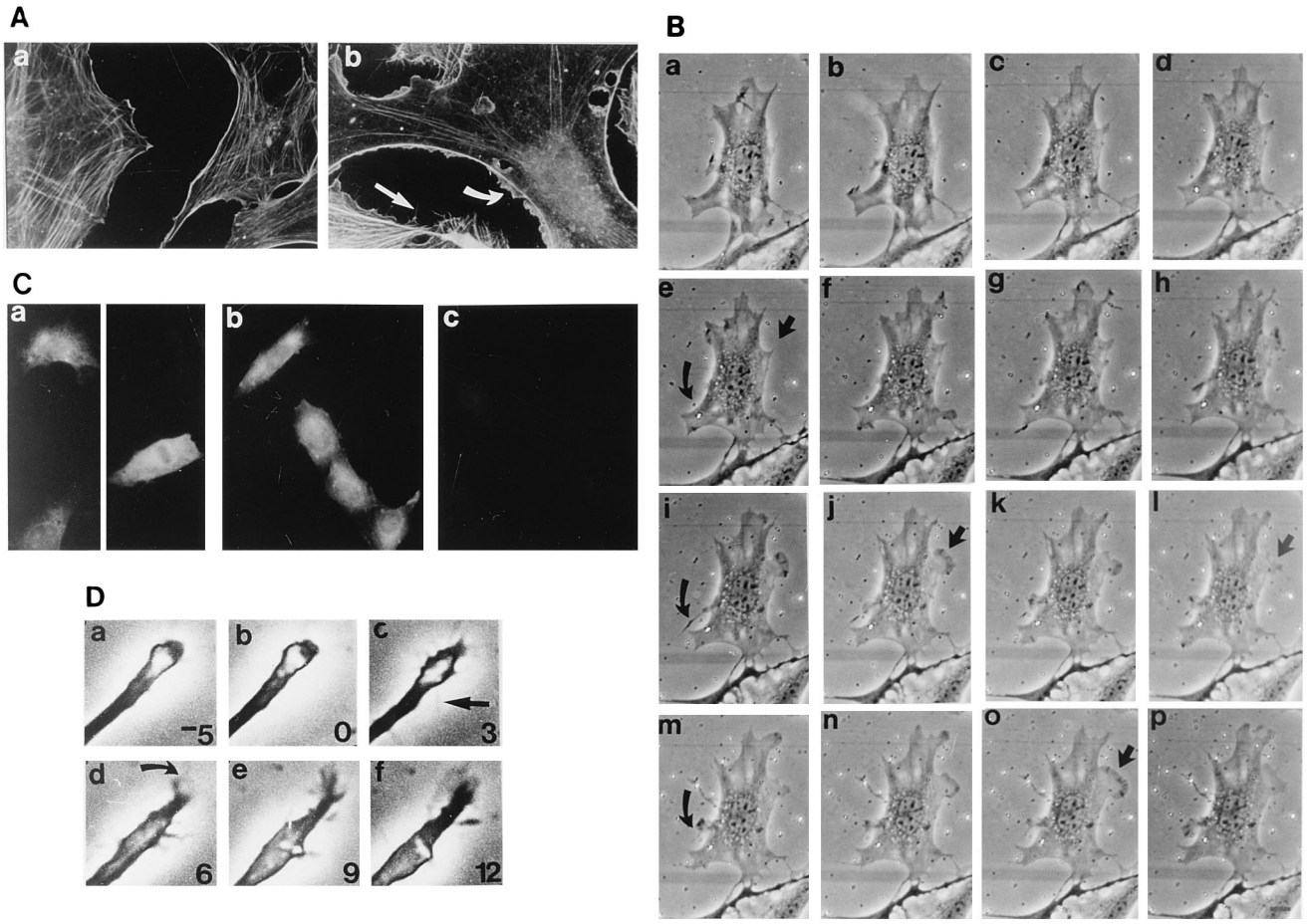


FIG. 2. *n*-Chimaerin induces the formation of the actin-based structures lamellipodia and filopodia. (A) Serum-starved Swiss 3T3 cells were microinjected with buffer only (a) or 0.5 mg of full-length *n*-chimaerin per ml (b). Cells were incubated for 10 min at 37°C and then fixed and stained with rhodamine-conjugated phalloidin to identify F-actin. The straight arrow indicates an example of peripheral-actin microspikes, while the curved arrow indicates a region undergoing membrane ruffling. Bar, 10 μm. (B) Formation and cycling of filopodia and of membrane ruffles and lamellipodia by *n*-chimaerin. Serum-starved Swiss 3T3 cells were microinjected with 1 mg of full-length *n*-chimaerin per ml at 0 min (a) and monitored by phase-contrast microscopy at 37°C at 2-min intervals for a total of 30 min (b to p). Note straight arrows in panels e, j, l, and o indicating the cycling (formation and decline) of a lamellipodium; curved arrows in panels e, i, and m indicate the formation of a filopodium followed by lamellipodium formation and membrane ruffling. Bar, 10 μm. (C) *n*-Chimaerin induces pinocytosis. Log-phase Swiss 3T3 cells were microinjected with proteins at 0.5 mg/ml before incubation with lucifer yellow for 1.5 h at 37°C. They were then washed, fixed, and observed by fluorescence microscopy. Cells were microinjected with Rac1 (a), full-length *n*-chimaerin (b), or BSA (c). (D) *n*-Chimaerin induces the formation of filopodia and lamellipodia in growth cones. The growth cones of serum-starved neuroblastoma N1E-115 cells were observed under phase-contrast microscopy for basal activity for 5 min (a and b) before being microinjected at 0 min with *n*-chimaerin and photographed at 3-min intervals (c to f). The arrow in panel c indicates a new filopodium, and the curved arrow in panel d indicates early lamellipodial formation. Times (in minutes) before and after microinjection are indicated at the bottoms of the panels.

specific downregulator of the Rac1 pathway. A variety of growth factors cause membrane ruffling, which can be inhibited by a dominant negative mutant Rac1 protein, $Rac1^{T17N}$ (46). These findings have established a role for Rac1 in membrane ruffling, but as the mode of action of dominant negative $Rac1^{T17N}$ is still not clear, it is not known whether this involves the increased formation of activated Rac1-GTP. Cells were injected with the GAP domain before treatment with a variety of agents, including phorbol ester (phorbol myristate acetate [PMA]; 100 nM [Fig. 1e and f]), 1-oleyl-2-acetyl-rac-glycerol (1 μg/ml [Fig. 1g and h]), platelet-derived growth factor (6 ng/ml), epidermal growth factor (10 ng/ml), bombesin (10 nM), and insulin (1 μg/ml). In all cases the factor-induced membrane ruffling was prevented by injection of the GAP domain. This suggests that these factors induce membrane ruffling by causing an increase in Rac1-GTP levels.

**Full-length *n*-chimaerin induces the formation of lamellipodia and filopodia.** Having established that the GAP domain is a downregulator of the Rac1 pathway, we wanted to determine the effect of full-length *n*-chimaerin on cell morphology. Strikingly, microinjection of full-length *n*-chimaerin induced membrane ruffling and formation of peripheral-actin microspikes within 5 to 10 min (Fig. 2A). The formation of these actin-containing structures continued for up to a few hours and then declined. In contrast, control cells (including those injected with BSA, thrombin-containing buffer, or factor $X_a$-containing buffer) have mainly smooth peripheral-actin staining (Fig. 2A). *n*-Chimaerin also induced a significant reduction in the number of stress fibers after 30 min (data not shown). To investigate the dynamics of the effects of *n*-chimaerin on cell morphology, time-lapse phase-contrast microscopy was used. Microinjection of *n*-chimaerin resulted in the formation of membrane ruffles (seen as darkened cell edges under phase-contrast microscopy), lamellipodia, and filopodia (Fig. 2B). Furthermore, we observed a cycling of changes in morphology whereby filopodia and lamellipodia formed, disappeared, and

reformed. *n*-Chimaerin was also found to induce pinocytosis to levels similar to those seen with Rac1 injection (Fig. 2C). As the formation of lamellipodia and filopodia is essential for growth cone development, we examined whether *n*-chimaerin could play a role in this process. Following microinjection of *n*-chimaerin into the bodies of serum-starved neuroblastoma N1E-115 cells, we observed a dramatic increase of new filopodial and lamellipodial activity at the growth cone (Fig. 2D). The microinjection of Cdc42Hs and Rac1 into these neuroblastoma cells also induced the formation of filopodia and lamellipodia, respectively (data not shown), as previously observed with Swiss 3T3 fibroblasts (27). In contrast to the use of full-length *n*-chimaerin, microinjection with truncated forms, including the C-terminal GAP domain (Δ1–105), the C-terminal GAP domain with a loss of GAP activity (Δ1–105/Δ131–133), or N-terminal chimaerin (Δ173–299), did not stimulate formation of filopodia or lamellipodia. Thus, only full-length *n*-chimaerin caused changes in cell morphology consistent with simultaneous activation of Rac1 and Cdc42Hs signalling pathways in both fibroblasts and neuroblastoma cells.

**Rho-GDI inhibits the morphological changes induced by *n*-chimaerin.** As Rho-GDI prevents Cdc42Hs, Rac1, and RhoA from interacting with GAPs (12, 20, 21), it was used to determine whether *n*-chimaerin requires any of these p21 proteins to induce changes in morphology. *n*-Chimaerin was coinjected with Rho-GDI, and the cells were subsequently stained with phalloidin. Rho-GDI not only blocked the effects of *n*-chimaerin but also reduced phalloidin staining in general (Fig. 3A; compare panels a and d).

***n*-Chimaerin-mediated induction of lamellipodia and filopodia requires active Rac1 and Cdc42Hs.** To determine whether the inductive effect of *n*-chimaerin on lamellipodium formation and pinocytosis and on filopodium formation involved Rac1 and Cdc42Hs, we coinjected *n*-chimaerin with dominant negative $Rac1^{T17N}$ or $Cdc42Hs^{T17N}$ protein. These mutant proteins specifically block growth factor-induced morphological changes acting through endogenous Rac1 and Cdc42Hs, respectively (27, 46). They are thought to function by titrating out specific activating factors, possibly GDP/GTP exchange factors (15, 16, 36, 49). $Rac1^{T17N}$ blocked membrane ruffling (Fig. 3A; compare panels a and b), lamellipodium formation (Fig. 3B; compare panels a and b), and pinocytosis (Fig. 3C) induced by *n*-chimaerin but not filopodium or microspike formation, while $Cdc42Hs^{T17N}$ blocked actin microspike (Fig. 3A; compare panels a and c) and filopodium (Fig. 3B; compare panels c and d) formation but not lamellipodium formation or membrane ruffling. Quantification of these results is depicted in Fig. 4, which also shows a general dose dependence for the induction of filopodia and lamellipodia by *n*-chimaerin injection. These results indicate that the morphological effects elicited by *n*-chimaerin required the participation of Rac1 and Cdc42.

We have previously shown that the deletion mutant Δ143–145 has impaired Rac1-binding and Rac1-GAP activity (6). When microinjected into cells, this mutant did not promote the morphological effects elicited with wild-type protein (Fig. 4). Thus, to exert its effects chimaerin needs to interact with the p21 proteins, although this experiment does not establish which of the two impairments in the mutant is responsible for the loss of stimulatory function. However, microinjection of another *n*-chimaerin mutant, Δ131–133, which has no GAP activity and yet still binds strongly to the p21 proteins (6), resulted in the induction of both filopodia and membrane ruffling (data not shown). Taken together, these results indicate that p21 binding, but not GAP activity, is required for full-length *n*-chimaerin to induce morphological changes.

**Phorbol ester inhibits *n*-chimaerin from inducing changes in cell morphology.** Since *n*-chimaerin GAP activity is stimulated in vitro by phorbol esters (5), we used PMA to attempt to downregulate Rac1 or Cdc42Hs signalling in cells to determine how this affected *n*-chimaerin's inductive properties. PMA treatment of cells on its own induces membrane ruffling (46), while microinjection of *n*-chimaerin on its own both induces membrane ruffling and lamellipodium formation and induces promotion of filopodia. When PMA was added to cells previously microinjected with *n*-chimaerin, the result was a loss of existing and inhibition of formation both of membrane ruffles and lamellipodia and of filopodia (Fig. 5). In contrast, microinjection of the mutant *n*-chimaerin (Δ143–145) without GAP activity did not affect the ability of PMA to induce membrane ruffling and lamellipodium formation (data not shown). LPA, a stress fiber-inducing agent, inhibits *n*-chimaerin GAP activity in vitro (5). Treatment of cells with either LPA or 0.5% FCS did not affect the ability of microinjected *n*-chimaerin to promote its morphological effects (Fig. 5c and d). These results suggest that the effects of microinjected *n*-chimaerin in promoting filopodium and lamellipodium formation are not achieved through its GAP activity. Rather, under conditions in which its GAP activity is stimulated, *n*-chimaerin acts as a downregulator, as previously shown by using the active C-terminal GAP domain.

***n*-Chimaerin colocalizes in situ with F-actin.** To determine its cellular localization, Swiss 3T3 cells were microinjected with *n*-chimaerin and then subjected to in situ double staining with anti-*n*-chimaerin antibodies and rhodamine-conjugated phalloidin. *n*-Chimaerin colocalized in situ with the F-actin structures and in particular membrane ruffles and peripheral-actin microspikes which had been induced (Fig. 6A, panels a to d). However, the injected C-terminal GAP domain (Δ1–105) showed a general diffuse cellular staining (Fig. 6A, panels e and f), suggesting that the N-terminal domain of *n*-chimaerin determines its colocalization with F-actin.

To investigate the requirement of the N terminus of *n*-chimaerin for its localization, we transfected COS7 cells with vectors encoding three different *n*-chimaerin proteins: full-length protein (pMT2-NC), protein with only the N-terminal 172 amino acids (pMT2-NCΔ173–330), and protein with the first 35 amino acid residues deleted (pMT2-NCΔ1–35). Cellular material was fractionated with or without the addition of Triton X-100 detergent and analyzed with anti-*n*-chimaerin antibodies by Western analysis. The majority of full-length *n*-chimaerin was insoluble even after extraction with detergent (Fig. 6B, lanes 5 to 8), as was the N-terminal (Δ173–330) *n*-chimaerin (Fig. 6B, lanes 9 to 12). However, pMT2-NCΔ1–35 was mainly detergent soluble (Fig. 6B, lanes 13 to 16). This construct also resulted in the synthesis of a C-terminal 20-kDa portion (established by domain-specific antibodies) of *n*-chimaerin ($p20^{nc}$), as a result of either internal initiation or proteolysis. This protein was located in the soluble fraction even without the addition of detergent (Fig. 6B, lanes 13 and 14). The results suggest that the N-terminal 172 amino acids of *n*-chimaerin are sufficient, and the first 35 amino acids are required, to allow a cytoskeletal localization of the protein.

***n*-Chimaerin induces a redistribution of vinculin.** As we had observed a loss of stress fibers following microinjection of both Rac1 and Cdc42Hs (27) and also following the microinjection of *n*-chimaerin, we next looked for effects on focal adhesion plaques which mark the ends of stress fibers (45). Cells were microinjected with *n*-chimaerin or control proteins and double stained with phalloidin and antivinculin antibodies; vinculin is a component of focal adhesion plaques. Within 10 min of microinjection with *n*-chimaerin, we observed a redistribution

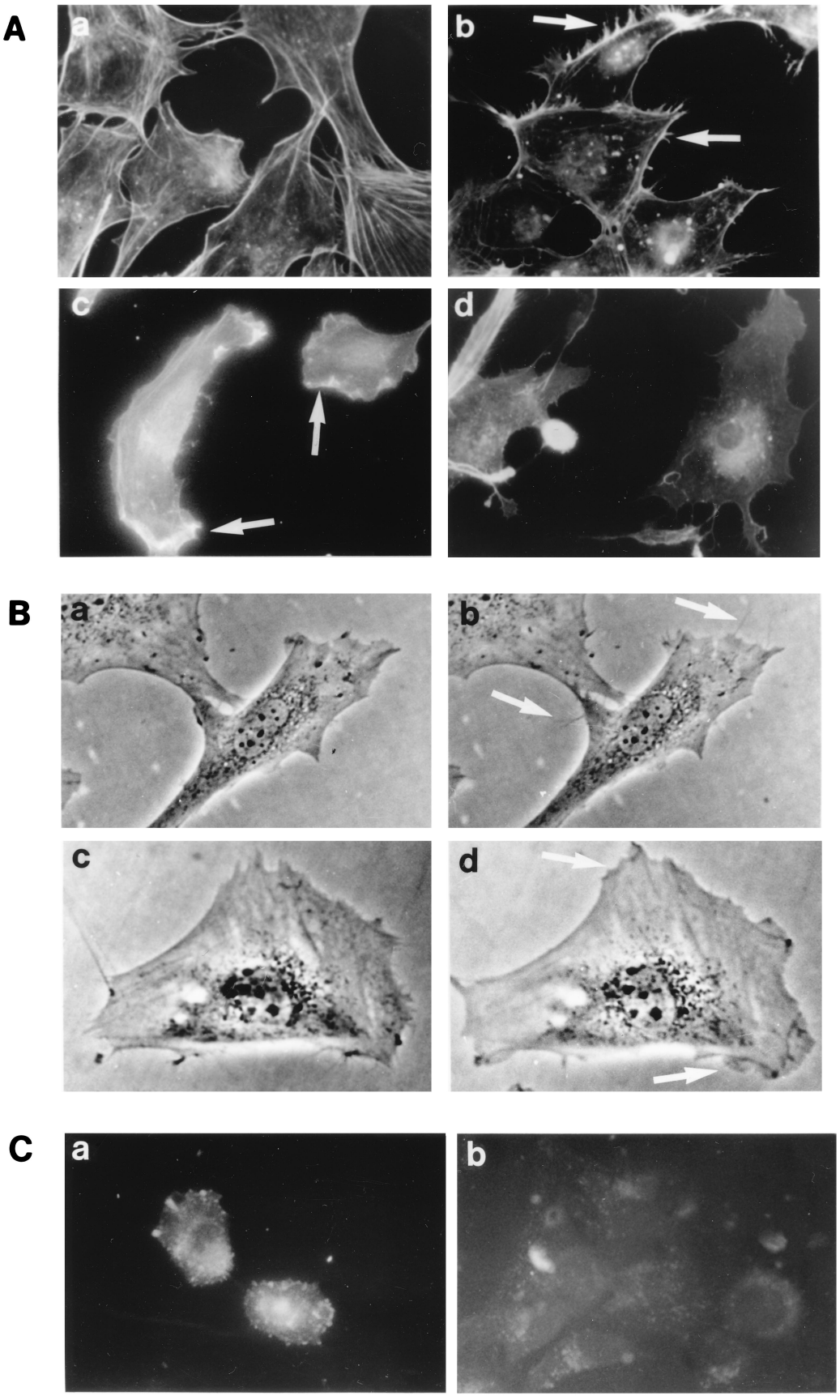
A
a
b
c
d
B
a
b
c
d
C
a
b

FIG. 3. Rac1 and Cdc42Hs are required for *n*-chimaerin's effects on cell morphology and pinocytosis. (A) Phalloidin staining of microinjected serum-starved cells. Cells were injected with buffer (a), *n*-chimaerin coinjected with $Rac1^{T17N}$ (b), *n*-chimaerin coinjected with $Cdc42Hs^{T17N}$ (c), or *n*-chimaerin coinjected with Rho-GDI (d). After a 10-min incubation at 37°C, cells were fixed and stained with rhodamine-conjugated phalloidin to detect F-actin. *n*-Chimaerin was injected at 0.5 mg/ml; $Rac1^{T17N}$, $Cdc42Hs^{T17N}$, and Rho-GDI were injected at 1 mg/ml. Panel d was exposed 50% more than other panels. All cells in the field were injected. Note the formation of microspikes in panel b and the formation of membrane ruffles in panel c, indicated by arrows. (B) Phase-contrast time-lapse microscopy analysis of microinjected serum-starved Swiss 3T3 cells. Full-length *n*-chimaerin was coinjected with dominant negative $Rac1^{T17N}$ into cells at 0 min (a) and after 5 min (b). Note production of filopodia (examples indicated by arrows). *n*-Chimaerin was coinjected with dominant negative $Cdc42Hs^{T17N}$ into cells at 0 min (c) and after 5 min (d). Note extension of lamellipodia and cell spreading (examples indicated by arrows). Proteins were each injected at 0.5 mg/ml. (C) Pinocytosis indicated by lucifer yellow uptake of microinjected log-phase cells. Cells were injected with *n*-chimaerin (a) and *n*-chimaerin coinjected with dominant negative $Rac1^{T17N}$ (b). Proteins were each injected at 0.5 mg/ml.

of vinculin staining, which was now associated with newly formed peripheral-actin microspikes up to their extremities (Fig. 7). This relocalization of vinculin probably represents newly formed multimolecular complexes (9, 39). These results suggest that *n*-chimaerin may participate in the formation of multimolecular complexes at the cell periphery associated with the generation of filopodia and lamellipodia.

## DISCUSSION

**Cellular effects of the *n*-chimaerin GAP domain.** In the present study, we wanted to establish whether the Rac1 and Cdc42Hs GAP *n*-chimaerin affects cellular morphology. To this end, *n*-chimaerin and N- and C-terminal domains, purified as recombinant proteins from *E. coli*, were microinjected into Swiss 3T3 fibroblasts and neuroblastoma cells and cell morphology was monitored. The GAP domain of *n*-chimaerin was found to act as a specific downregulator of the Rac1 pathway, probably by stimulating the intrinsic Rac1-GTPase activity. Microinjection of the GAP domain eliminated growth factor-mediated membrane ruffling and lamellipodium formation in serum-starved cells. We conclude, therefore, that growth factors activate Rac1 by causing an increase in the levels of Rac1-GTP and that this results in membrane ruffling and lamellipodium formation.

**Cellular effects of full-length *n*-chimaerin.** Microinjection of full-length *n*-chimaerin into Swiss 3T3 and neuroblastoma cells induced the formation of lamellipodia and filopodia and stimulated pinocytosis, in contrast to the effects of the GAP domain. All truncated forms of *n*-chimaerin, including the GAP domain, the GAP-deficient GAP domain (*n*-chimaerin mutant Δ1–105/Δ131–133), and the N-terminal domain alone, were ineffective in simulating the effects obtained by injection of full-length *n*-chimaerin. Thus, *n*-chimaerin requires both the GAP domain, with its p21-binding property, and the N-terminal domain, necessary for localization, to induce lamellipodia and filopodia. These effects of *n*-chimaerin, involving the simultaneous activation of the Rac1 and Cdc42Hs pathways, contrast with those obtained by either injection of Cdc42Hs

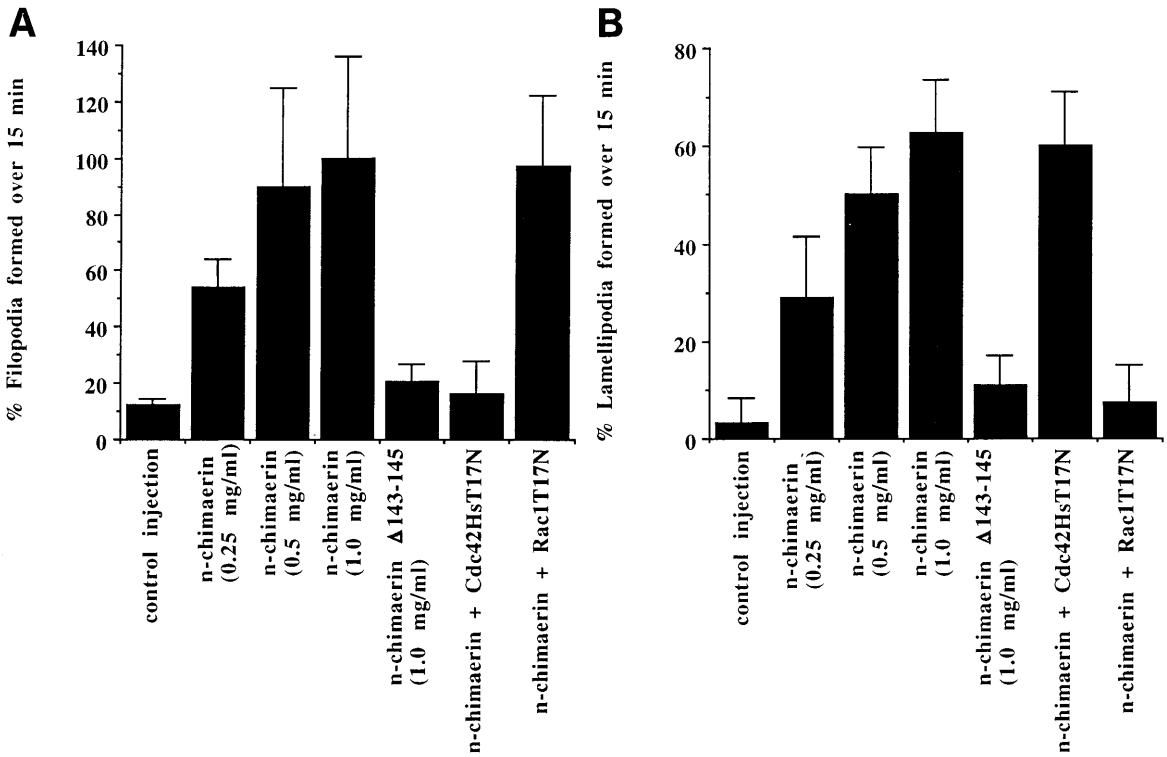


FIG. 4. Quantification and specificity of filopodium and lamellipodium formation promoted by *n*-chimaerin. Serum-starved Swiss 3T3 cells were injected with proteins as indicated, and the cells were monitored by time-lapse phase-contrast microscopy for new filopodial and lamellipodial formation over a 15-min period. (A) Filopodium formation, expressed as the percentage of those induced by injection of 1 mg of *n*-chimaerin per ml (100%). (B) Induction of lamellipodia, estimated as the percentage of cell edges to undergo formation of lamellipodia. For coinjection experiments, a 1-mg/ml concentration of each *n*-chimaerin and dominant negative Rac1 or Cdc42Hs protein was used. *n*, 10 to 16. Standard deviations are shown by error bars.

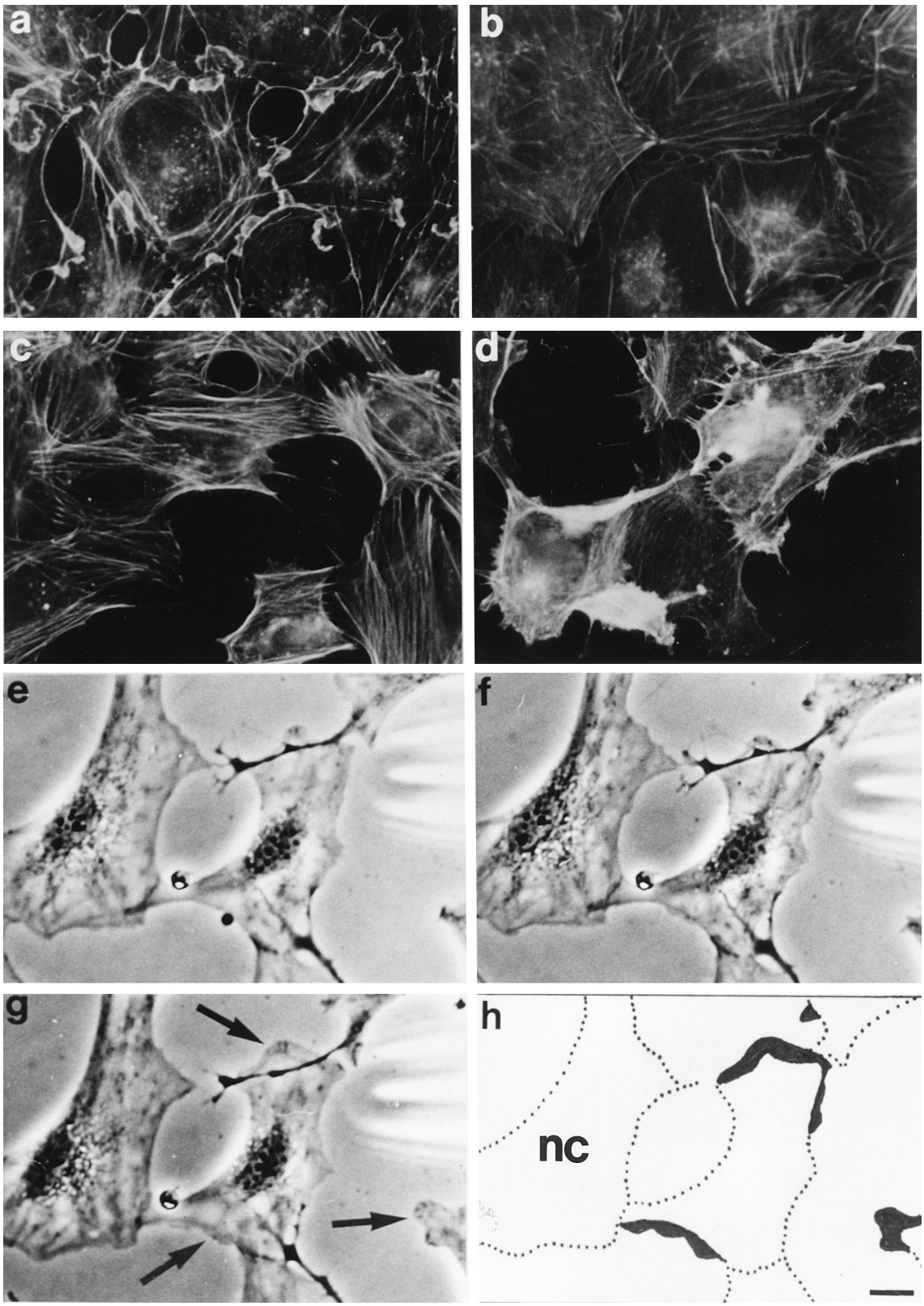


FIG. 5. Treatment of cells with phorbol ester inhibits *n*-chimaerin-induced changes in cell morphology. Cells in panels a to d were incubated at 37°C for 10 min after treatment before being fixed and stained with rhodamine-conjugated phalloidin to identify F-actin. (a) Cells treated with 100 nM PMA; (b) cells microinjected with *n*-chimaerin (0.5 mg/ml) and then treated with PMA; (c) cells treated with 0.5% FCS; (d) cells microinjected with *n*-chimaerin (0.5 mg/ml) and then treated with 0.5% FCS. Cells in panels e to h were monitored by phase-contrast time-lapse microscopy. The cell in the left portion of the field was microinjected with *n*-chimaerin (0.5 mg/ml) before being treated with 100 nM PMA at 0 min (e), 5 min (f), and 10 min (g). (h) Schematic diagram of panels e to g with cell microinjected with *n*-chimaerin (nc). Note lamellipodial extensions in cells on the right which were not microinjected, indicated by arrows, and by filled-in areas in panel h. Bar, 10 μm.

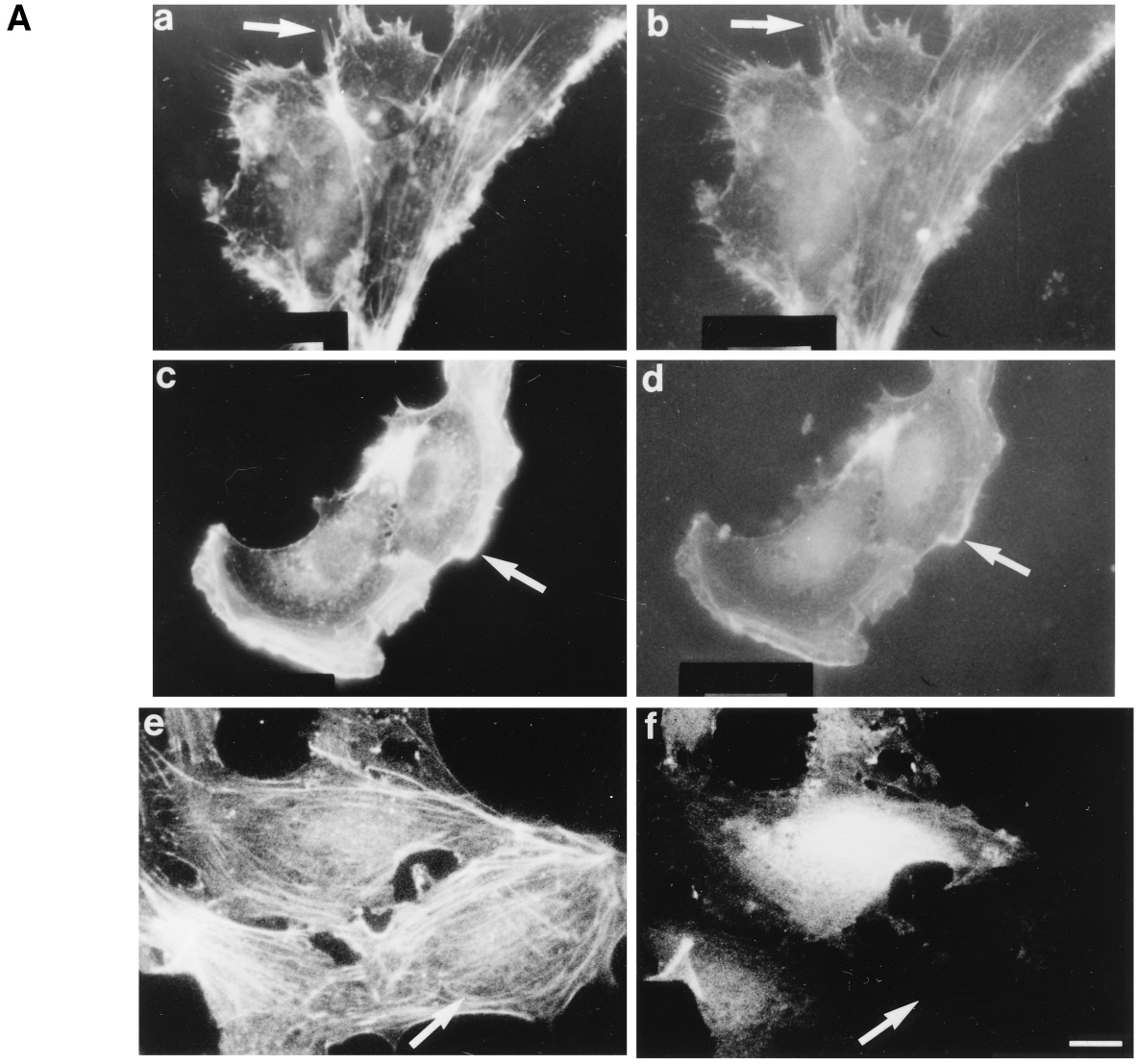


FIG. 6. *n*-Chimaerin colocalizes with F-actin in situ. (A) Cells were microinjected and incubated at 37°C for 1 h before being fixed and then double stained with rabbit anti-*n*-chimaerin antibodies followed by fluorescein isothiocyanate-conjugated anti-rabbit antibodies (b, d, and f) and rhodamine-conjugated phalloidin (a, c, and e). Cells were microinjected with full-length *n*-chimaerin (a to d) or the GAP domain (Δ1–105) (e and f). Note arrows in panels a and b indicating *n*-chimaerin locating at actin microspikes. Arrows in panels c and d indicate *n*-chimaerin locating at membrane ruffles; the arrow in panel f indicates background antibody staining of a noninjected cell. Bar, 10 μm. (B) Extracts from COS7 cells transfected with control pMT2 (lanes 1 to 4) and *n*-chimaerin-expressing constructs: pMT2-NC encoding full-length *n*-chimaerin (lanes 5 to 8), pMT2-NCΔ173–330 encoding N-terminal *n*-chimaerin (lanes 9 to 12), and pMT2-NCΔ1–35 encoding *n*-chimaerin with the first 35 amino acids absent (lanes 13 to 16). Cell extracts were made either with (+) or without (−) the detergent Triton X-100. Samples were either the supernatants (S) or the pellets (P). After centrifugation, samples were run out by SDS-polyacrylamide gel electrophoresis, transferred to nitrocellulose by dry blotting, and probed with *n*-chimaerin-specific antibodies. Arrows indicate sizes (in kilodaltons) of expressed proteins. Note that COS7 cells do not express endogenous *n*-chimaerin.

into, or bradykinin treatment of, fibroblasts in which a hierarchy with initial activation of Cdc42Hs followed sequentially by Rac1 activation was observed (27, 39). The inductive effects of *n*-chimaerin required the active participation of Rac1 and Cdc42Hs since coinjection with dominant negative mutants $Rac1^{T17N}$ and $Cdc42Hs^{T17N}$ blocked lamellipodium and filopodium formation, respectively. The *n*-chimaerin mutant Δ131–133 (6), which is GAP defective but has strong p21-binding activity, was able to induce these structures, indicating that p21 binding but not GAP activity is required for this function of *n*-chimaerin. This requirement is also reflected by the inability of the *n*-chimaerin mutant Δ143–145, which is defective both in p21 binding and GAP activities, to induce these morphologies. We have previously observed that microinjection with Cdc42Hs leads to the loss of stress fibers concomitantly with

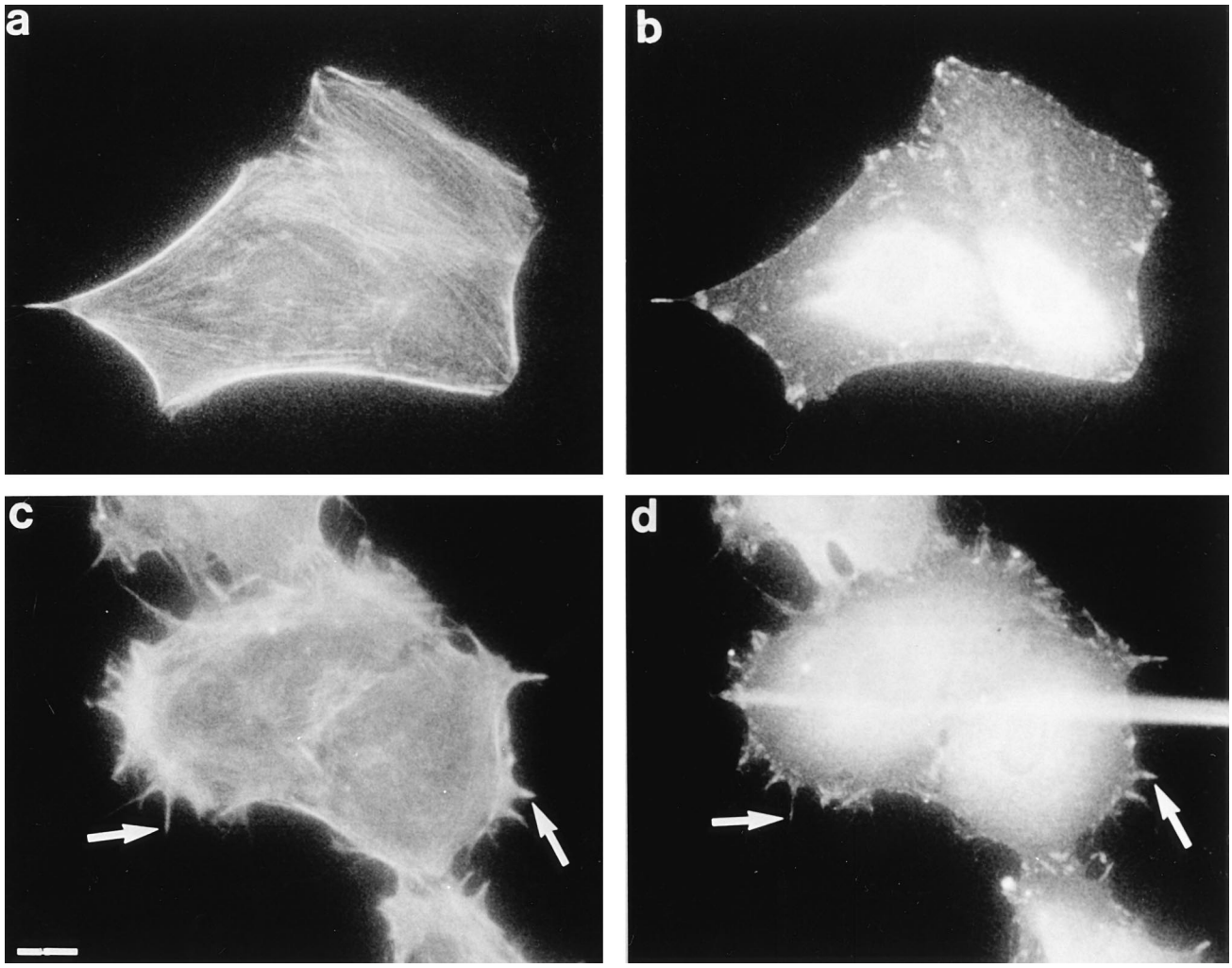


FIG. 7. *n*-Chimaerin promotes a redistribution of the focal adhesion protein vinculin. Cells were microinjected and incubated at 37°C for 10 min before being fixed and double stained with rabbit antivinculin antibodies followed by rhodamine-conjugated phalloidin (a and c) and fluorescein isothiocyanate-conjugated anti-rabbit antibodies (b and d). Cells were microinjected with control buffer (a and b) or 0.5 mg of *n*-chimaerin per ml (c and d). Note arrows in panels c and d indicating vinculin staining in peripheral-actin microspikes. Bar, 10 μm.

the formation of peripheral-actin microspikes (27), while others have described stress fiber loss following transfection with *n*-chimaerin cDNA (22). We also observed a loss of stress fibers following microinjection with *n*-chimaerin, concurrently with formation of lamellipodia and filopodia. This loss was accompanied not only by a loss of focal adhesion plaques as revealed by vinculin staining but also by redistribution of vinculin to newly formed peripheral-actin sites. This chimaerin-induced relocalization of vinculin is likely to represent the formation of Cdc42Hs- and Rac1-type multimolecular complexes (9, 39).

*n*-Chimaerin behaved as a downregulator in the presence of PMA, which is predicted from in vitro experiments to activate its GAP activity. Thus, although PMA treatment of serum-starved cells induced membrane ruffling and lamellipodium formation, this was not seen in cells preinjected with *n*-chimaerin. As predicted from these results, PMA also failed to induce membrane ruffling in N1E-115 neuroblastoma cells which express endogenous chimaerin (results not shown). PKC activation, following PMA treatment, is not likely to be a common signal transducing element in the induction of lamellipodia because some factors cause lamellipodium formation without activating PKC whereas other factors activate PKC without inducing lamellipodia (47, 53). It is not clear yet how PMA could function to block all of the activities stimulated by *n*-chimaerin. In PMA-treated cells, *n*-chimaerin appears not only to downregulate Rac1 activity but also to no longer activate Cdc42Hs, as no filopodium formation was observed. This lack of filopodium-inducing activity does not necessitate a Cdc42Hs-GAP activity for *n*-chimaerin, although this would be sufficient to explain it. It may be that in the presence of activators *n*-chimaerin no longer interacts with Cdc42Hs.

**Localization of *n*-chimaerin.** The cellular localization of *n*-chimaerin was examined by in situ immunofluorescence of microinjected cells. *n*-Chimaerin colocalized with F-actin, and staining was clearly evident in peripheral-actin microspikes and membrane ruffles. In contrast, the GAP domain, lacking the N terminus, did not colocalize with F-actin but gave a more diffuse staining, which is consistent with a general cytoplasmic location. It is possible that *n*-chimaerin binds to both structured and nonstructured actin microfilaments, with its association with the latter facilitating formation of Rac1- and

Cdc42Hs-dependent structures on recruitment of the GTPases. Although the N terminus is required for localization of *n*-chimaerin to the cytoskeleton, it is not yet clear whether *n*-chimaerin binds directly to actin or to an actin-binding protein.

**Conclusion.** *n*-Chimaerin, which requires the activity of Rac1 and Cdc42Hs to induce formation of filopodia and lamellipodia, binds Rac1 preferably in the GTP form (6) and the Cdc42Hs GTPase-negative mutant (42). The ability of the *n*-chimaerin mutant Δ131–133 (lacking GAP activity) but not mutant Δ143–145 (deficient in both GAP and p21-binding activities) to induce changes in cellular morphology strongly suggests that p21-binding activity is required for *n*-chimaerin to function. Presently, we do not know the exact mechanism whereby *n*-chimaerin induces Cdc42Hs- and Rac1-type morphologies, although there are several potential modes of action. One possibility is that *n*-chimaerin acts as a cytoskeletal receptor for activated Cdc42Hs and Rac1, whose recruitment along with other components facilitates morphological reorganization. Another possibility is that *n*-chimaerin activates Rac1 and Cdc42Hs exchange factors, or recruits them to the actin cytoskeleton, to bring about activation of the two p21 proteins. However, microinjection of GDP-bound Rac1 or Cdc42Hs protein into Swiss 3T3 fibroblasts is as potent as injection of GTP-bound forms in inducing rapid morphological changes, suggesting that exchange activity is not limiting.

*n*-Chimaerin's potential role is most clearly seen with its microinjection into neuroblastoma cells, which results in lamellipodium and filopodium formation at the leading edge of growth cones. As *n*-chimaerin mRNA is found in neurons and expression increases during development at the time of extensive neural plasticity, synaptogenesis, and cellular differentiation (32), our results are consistent with the notion that it may function to bring about coordinated morphological changes involved in these events. Cycles of filopodium and lamellipodium formation, similar to those induced by *n*-chimaerin, occur in both fibroblasts and neuroblastoma cells, in which these events underpin cell motility (7, 11, 40, 51, 52). Although *n*-chimaerin itself is not expressed in Swiss 3T3 fibroblasts, it is possible that they contain an endogenous homologous protein since other forms of chimaerin are found in nonneuronal cells, including β-chimaerin in testis cells (30) and γ-chimaerin in lymphocytes (31). Our results suggest that *n*-chimaerin allows simultaneous activation of the Rac1 and Cdc42Hs signalling pathways, which may be important for rapid remodelling of cells during migration and growth cone development.

## ACKNOWLEDGMENT

We appreciate the support of the Glaxo-Singapore Research Fund.

## REFERENCES


1. **Adams, A. E. M., D. I. Johnson, R. M. Longnecker, B. F. Sloat, and J. R. Pringle.** 1990. CDC42 and CDC43, two additional genes involved in budding and the establishment of cell polarity in the yeast Saccharomyces cerevisiae. J. Cell Biol. **111:**131–142.
2. **Ahmed, S., R. Kozma, C. Hall, and L. Lim.** 1995. GAP activity of n-chimaerin and effects of lipids. Methods Enzymol. **256:**114–125.
3. **Ahmed, S., R. Kozma, J. Lee, C. Monfries, N. Harden, and L. Lim.** 1991. The cysteine-rich domain of human proteins, neuronal chimaerin, protein kinase C and diacylglycerol kinase binds zinc. Evidence for the role of a zinc-dependent structure in phorbol ester binding. Biochem. J. **280:**233–241.
4. **Ahmed, S., R. Kozma, C. Monfries, C. Hall, H. H. Lim, P. Smith, and L. Lim.** 1990. Human brain n-chimaerin cDNA encodes a novel phorbol ester receptor. Biochem. J. **272:**767–773.
5. **Ahmed, S., J. Lee, R. Kozma, A. Best, C. Monfries, and L. Lim.** 1993. A novel functional target for tumor-promoting phorbol esters and lysophosphatidic acid. The p21rac-GTPase activating protein n-chimaerin. J. Biol. Chem. **268:** 10709–10712.
6. **Ahmed, S., J. Lee, L.-P. Wen, Z. Zhao, J. Ho, A. Best, R. Kozma, and L. Lim.** 1994. Breakpoint cluster region gene product-related domain of n-chimaerin. J. Biol. Chem. **269:**17642–17648.
7. **Aletta, J. M., and L. A. Greene.** 1988. Growth cone configuration and advance: a time-lapse study using video-enhanced differential interference contrast microscopy. J. Neurosci. **8:**1425–1435.
8. **Boguski, M. S., and F. McCormick.** 1993. Proteins regulating Ras and its relatives. Nature (London) **366:**643–654.
9. **Burridge, K., K. Fath, T. Kelly, G. F. Nuckolls, and C. Turner.** 1988. Focal adhesions: transmembrane junctions between the extracellular matrix and the cytoskeleton. Annu. Rev. Cell Biol. **4:**487–525.
10. **Cantor, S. B., T. Urano, and L. A. Feig.** 1995. Identification and characterization of Ral-binding protein 1, a potential downstream target of Ral GTPases. Mol. Cell. Biol. **15:**4578–4584.
11. **Chien, C.-B., D. E. Rosenthal, W. A. Harris, and C. E. Holt.** 1993. Navigational errors made by growth cones without filopodia in the embryonic xenopus brain. Neuron **11:**237–251.
12. **Chuang, T. H., X. Xu, U. G. Knaus, M. J. Hart, and G. M. Bokoch.** 1993. GDP dissociation inhibitor prevents intrinsic and GTPase activating protein-stimulated GTP hydrolysis by the Rac GTP-binding protein. J. Biol. Chem. **268:**775–778.
13. **Diekmann, D., S. Brill, M. D. Garrett, N. Totty, J. Hsuan, C. Monfries, C. Hall, L. Lim, and A. Hall.** 1991. Bcr encodes a GTPase-activating protein for p21rac. Nature (London) **351:**400–402.
14. **Drubin, D. G.** 1991. Development of cell polarity in budding yeast. Cell **65:** 1093–1096.
15. **Farnsworth, C. L., and L. A. Feig.** 1991. Dominant inhibitory mutations in the $Mg^{2+}$-binding site of $Ras^{H}$ prevent its activation by GTP. Mol. Cell. Biol. **11:**4822–4829.
16. **Feig, L. A., and G. M. Cooper.** 1988. Inhibition of NIH 3T3 cell proliferation by a mutant *ras* protein with preferential affinity for GDP. Mol. Cell. Biol. **8:** 3235–3243.
17. **Guan, K. L., and J. E. Dixon.** 1991. Eukaryotic proteins expressed in E. coli: an improved thrombin cleavage and purification procedure of fusion proteins with glutathione S-transferase. Anal. Biochem. **192:**262–267.
18. **Hall, A.** 1994. Small GTP-binding proteins and the regulation of the actin cytoskeleton. Annu. Rev. Cell Biol. **10:**31–54.
19. **Hall, C., C. Monfries, P. Smith, H. H. Lim, R. Kozma, S. Ahmed, V. Vanniasingham, T. Leung, and L. Lim.** 1990. Novel human brain cDNA encoding a 34,000 Mr protein n-chimaerin, related to both the regulatory domain of protein kinase C and BCR, the product of the breakpoint cluster region gene. J. Mol. Biol. **211:**11–16.
20. **Hancock, J. F., and A. Hall.** 1993. A novel role for Rho-GDI as an inhibitor of GAP proteins. EMBO J. **12:**1915–1921.
21. **Hart, M. J., Y. Maru, D. Leonard, O. N. Witte, T. Evans, and R. A. Cerione.** 1992. A GDP-dissociation inhibitor that serves as a GTPase inhibitor for the Ras-like protein Cdc42Hs. Science **258:**812–815.
22. **Herrera, R., and B. D. Shivers.** 1994. Expression of α1-chimaerin (rac1 GAP) alters the cytoskeletal and adhesive properties of fibroblasts. J. Cell. Biochem. **56:**582–591.
23. **Homma, Y., and Y. Emori.** 1995. A dual functional signal mediator showing RhoGAP and phospholipase C stimulating activities. EMBO J. **14:**286–291.
24. **Isomura, M., A. Kikuchi, N. Ohga, and Y. Takai.** 1991. Regulation of binding of rhoB p20 to membranes by its specific regulatory protein, GDP dissociation inhibitor. Oncogene **6:**119–124.
25. **Johnson, D. I., and J. R. Pringle.** 1990. Molecular characterization of CDC42, a Saccharomyces cerevisiae gene involved in the development of cell polarity. J. Cell Biol. **111:**143–152.
26. **Kaufman, R. J., M. V. Davies, V. K. Pathak, and J. W. B. Hershey.** 1989. The phosphorylation state of eucaryotic initiation factor 2 alters translational efficiency of specific mRNAs. Mol. Cell. Biol. **9:**946–958.
27. **Kozma, R., S. Ahmed, A. Best, and L. Lim.** 1995. The Ras-related protein Cdc42Hs and bradykinin promote formation of peripheral actin microspikes and filopodia in Swiss 3T3 fibroblasts. Mol. Cell. Biol. **15:**1942–1952.
28. **Kwong, C. H., H. L. Malech, D. Rotrosen, and T. L. Leto.** 1993. Regulation of the human neutrophil NADPH oxidase by rho-related G-proteins. Biochemistry **32:**5711–5717.
29. **Laemmli, U. K.** 1970. Cleavage of structural proteins during the assembly of the head of bacteriophage T4. Nature (London) **227:**680–685.
30. **Leung, T., B. E. How, E. Manser, and L. Lim.** 1993. Germ-cell β-chimaerin, a new GTPase-activating protein for p21rac, is specifically expressed during the acrosomal assembly stage in rat testis. J. Biol. Chem. **268:**3813–3816.
31. **Leung, T., and L. Lim.** Unpublished data.
32. **Lim, H. H., G. J. Michael, P. Smith, L. Lim, and C. Hall.** 1992. Rat n-chimaerin, a p21rac GAP: cDNA sequence, developmental regulation and neuronal expression of its mRNA. Biochem. J. **287:**415–422.
33. **Manser, E., T. Leung, C. Monfries, M. Teo, C. Hall, and L. Lim.** 1992. Diversity and versatility of GTPase activating proteins for the p21rho subfamily of ras G proteins detected by a novel overlay assay. J. Biol. Chem. **267:** 16025–16028.
34. **Martin, G. A., A. Yatani, R. Clark, L. Conroy, P. Polakis, A. M. Brown, and F. McCormick.** 1992. GAP domains responsible for ras p21-dependent inhibition of muscarinic atrial $K^+$ channel currents. Science **255:**192–194.
35. **Maru, Y., and O. N. Witte.** 1991. The BCR gene encodes a novel serine/

threonine kinase activity within a single exon. Cell **67:**459–468.
36. **Medema, R. H., A. M. M. de Vries-Smits, G. C. M. van der Zon, J. A. Maassen, and J. L. Bos.** 1993. Ras activation by insulin and epidermal growth factor through enhanced exchange of guanine nucleotides on $p21^{ras}$. Mol. Cell. Biol. **13:**155–162.
37. **Miura, Y., A. Kikuchi, T. Musha, S. Kuroda, H. Yaku, T. Sasaki, and Y. Takai.** 1993. Regulation of morphology by rho p21 and its inhibitory GDP/GTP exchange protein (rho-GDI) in Swiss 3T3 cells. J. Biol. Chem. **268:**510–515.
38. **Munemitsu, S., M. A. Innis, R. Clark, F. McCormick, A. Ullrich, and P. Polakis.** 1990. Molecular cloning and expression of a G25K cDNA, the human homolog of the yeast cell cycle gene *CDC42*. Mol. Cell. Biol. **10:**5977–5982.
39. **Nobes, C. D., and A. Hall.** 1995. Rho, Rac and Cdc42 GTPases regulate the assembly of multi-molecular focal complexes associated with actin stress fibres, lamellipodia and filopodia. Cell **81:**53–62.
40. **O'Connor, T. P., and D. Bentley.** 1993. Accumulation of actin in subsets of pioneer growth cone filopodia in response to neural and epithelial guidance cues in situ. J. Cell Biol. **123:**935–948.
41. **Paterson, H. F., A. J. Self, M. D. Garratt, I. Just, K. Aktories, and A. Hall.** 1990. Microinjection of recombinant p21rho induces rapid changes in cell morphology. J. Cell Biol. **111:**1001–1007.
42. **Prigmore, E., S. Ahmed, R. Kozma, and L. Lim.** Unpublished data.
43. **Regazzi, R., K. Kikuchi, Y. Takai, and C. B. Wollheim.** 1992. The small GTP-binding proteins in the cytosol of insulin-secreting cells are complexed to GDP dissociation inhibitor proteins. J. Biol. Chem. **267:**17512–17519.
44. **Reinhard, J., A. A. Scheel, D. Diekmann, A. Hall, C. Ruppert, and M. Bahler.** 1995. A novel type of myosin implicated in signalling by rho family GTPases. EMBO J. **14:**697–704.
45. **Ridley, A. J., and A. Hall.** 1992. The small GTP-binding protein rho regulates the assembly of focal adhesions and actin stress fibres in response to growth factors. Cell **70:**389–399.
46. **Ridley, A. J., H. F. Paterson, C. Johnston, D. Diekmann, and A. Hall.** 1992. The small GTP-binding protein rac regulates growth factor-induced membrane ruffling. Cell **70:**401–410.
47. **Rozengurt, E.** 1989. Signal transduction pathways in mitogenesis. Br. Med. Bull. **45:**515–528.
48. **Sambrook, J., E. F. Fritsch, and T. Maniatis.** 1989. Molecular cloning: a laboratory manual, 2nd ed. Cold Spring Harbor Laboratory Press, Cold Spring Harbor, N.Y.
49. **Schweighoffer, F., H. Cai, M. C. Chevallier-Multon, I. Fath, G. Cooper, and B. Tocque.** 1993. The *Saccharomyces cerevisiae* SDC25 C-domain gene product overcomes the dominant inhibitory activity of Ha-Ras Asn-17. Mol. Cell. Biol. **13:**39–43.
50. **Shinjo, K., J. G. Koland, M. J. Hart, V. Narasimhan, D. I. Johnson, T. Evans, and R. A. Cerione.** 1990. Molecular cloning of the gene for the human placental GTP-binding protein $G_p$ (G25K): identification of this GTP-binding protein as the human homolog of the yeast cell-division-cycle protein CDC42. Proc. Natl. Acad. Sci. USA **87:**9853–9857.
51. **Stirling, R. V., and S. A. Dunlop.** 1995. The dance of the growth cones—where to next? Trends Neurosci. **18:**111–115.
52. **Tanaka, E., T. Ho, and M. W. Kirschner.** 1995. The role of microtubule dynamics in growth cone motility and axonal growth. J. Cell Biol. **128:**139–155.
53. **van Corven, E. J., A. Groenink, K. Jalink, T. Eichholtz, and W. H. Moolenaar.** 1989. Lysophosphatidate-induced cell proliferation: identification and dissection of signalling pathways mediated by G proteins. Cell **59:**45–54.
54. **Yatani, A., K. Okabe, P. Polakis, R. Halenbeck, F. McCormick, and A. M. Brown.** 1990. Ras p21 and GAP inhibit coupling of muscarinic receptors to atrial K+ channels. Cell **61:**769–776.